March 2008

# Rectification by charging: Contact-induced current asymmetry in molecular conductors

O D. Miller
*Univ Virginia, Dept Elect & Comp Engn*

Bhaskaran Muralidharan
*Purdue University*, bmuralid@purdue.edu

N Kapur
*Univ Virginia, Dept Chem Engn*

A W. Ghosh
*Univ Virginia, Dept Elect & Comp Engn*

# Rectification by charging: Contact-induced current asymmetry in molecular conductors

O. D. Miller,[1] B. Muralidharan,[2] N. Kapur,[3] and A. W. Ghosh[1]
[1]*Department of Electrical and Computer Engineering, University of Virginia, Charlottesville, Virginia 22904, USA*
[2]*School of Electrical and Computer Engineering and Network for Computational Nanotechnology, Purdue University, West Lafayette, Indiana 47906, USA*
[3]*Department of Chemical Engineering, University of Virginia, Charlottesville, Virginia 22904, USA*
(Received 23 July 2007; published 26 March 2008)

We outline the qualitatively different physics behind charging-induced current asymmetries in molecular conductors operating in the weakly interacting self-consistent field (SCF) and the strongly interacting Coulomb blockade (CB) regimes. The SCF conductance asymmetry originates in the asymmetric shifts of the closed-shell molecular conducting levels, driven by unequal mean-field potentials for positive and negative biases. A very different current asymmetry arises for CB due to the unequal number of open-shell excitation channels at opposite bias voltages. The CB regime, dominated by single charge effects, typically requires a computationally demanding many-electron or Fock-space description to do justice to its complex excitation spectrum. However, our analysis of molecular CB measurements reveals that many novel signatures can be explained using a simpler orthodox model that involves an incoherent sum of Fock-space excitations and hence treats the molecule as a metallic dot. This also reduces the complexity of the Fock-space description by including charge configurations alone, somewhat underscoring the richness of its electronic structure while retaining the essential single charge nature of the transport process. The inclusion of electronic structure with well-resolved Fock space excitations is, however, crucial in some notable examples.

DOI: 10.1103/PhysRevB.77.125427 PACS number(s): 73.22.−f, 73.23.−b, 73.40.Ei, 68.65.−k

## I. INTRODUCTION

Ever since its inception,[1] molecular rectification has remained of great scientific interest. While rectification could arise from intrinsic structural asymmetries, many experiments[2–5] exhibit pronounced asymmetries in current-voltage (*I-V*) or conductance-voltage (*G-V*) characteristics in relatively symmetric molecules unequally coupled to contacts. There are two classes of such asymmetries. For molecules strongly bonded with contacts, comparable current levels are reached over unequal voltage ranges [Fig. 1(a)], leading to prominent conductance asymmetries.[2] The asymmetry arises from the different charging energies that generate *unequal mean-field potentials* for opposite bias voltages.[6] Reducing the contact-molecular couplings drives the system into Coulomb blockade (CB), where even the heights of the intermediate open-shell current plateaus are asymmetric[7] [Fig. 1(b)]. This asymmetry has a different physical origin rooted in its many-body excitations, driven by the *unequal number of discrete spin addition and removal channels* at opposite bias. It is thus clear that the physics of rectification can depend sensitively on the strength of the electron-electron interaction.

The nonequilibrium Green's function (NEGF) formalism is widely established for quantum transport in the self-consistent field (SCF) regime[8] for a diverse variety of materials from nanoscale silicon transistors to nanowires, nanotubes, and spintronic elements. The ability to incorporate accurate quantum chemistry[9,10] through averaged potentials makes the NEGF-SCF scheme particularly attractive. However, this approach does not readily translate to the CB regime, even qualitatively.[11–13] While this limitation is well recognized by the quantum dot community,[14,15] it is relatively unappreciated in the molecular electronics world that has frequently invoked "first principles" theories based on restricted or unrestricted SCF potentials, even to address CB problems.[16–19] The CB regime, observed in molecules with weak contact coupling,[3–5] manifests clear signatures of single-electron charging, such as suppressed zero-bias conductances and abrupt jumps in current. The inherent difficulty in using the SCF theory for these systems arises from the fact that the open-shell current levels depend on full exclusion statistics in its many-body Fock space. Even for a minimal single-orbital model, it is easy to establish that while the open-shell current plateau *widths* depend on the correlation strengths, their *heights* are independent of the interaction strength, and in that sense, universal—a feature that even spin unrestricted SCF models fail to capture.[11] Transport in CB maps onto a rather difficult combinatorial problem in Fock space that cannot readily be projected *a priori* onto its one-particle SCF potential, even phenomenologically.

A proper treatment of the Fock-space excitations requires solving a set of master equations directly in the Fock space of the molecular many-body Hamiltonian.[11,14,15] A significant penalty is the increased computational cost that requires sacrificing the quantum chemical sophistication of *ab initio* models, in lieu of an exact treatment of the Coulomb interaction in simpler phenomenological models. Within such an exactly diagonalizable model, one can capture transport features which are quite novel and unique to the CB regime, such as inelastic cotunneling, gate-modulated current rectification, and Pauli spin blockade.[11,20,21] The presence of contact asymmetry makes these features even more intriguing, while somewhat simplifying the analysis by driving the system into equilibrium with the stronger contact.

The inadequacy of SCF models has already been elucidated in our earlier works.[11,12] The main focus of this paper is the elucidation of its specific experimental consequences

 

Asymmetric Current Widths

Asymmetric Plateau Heights

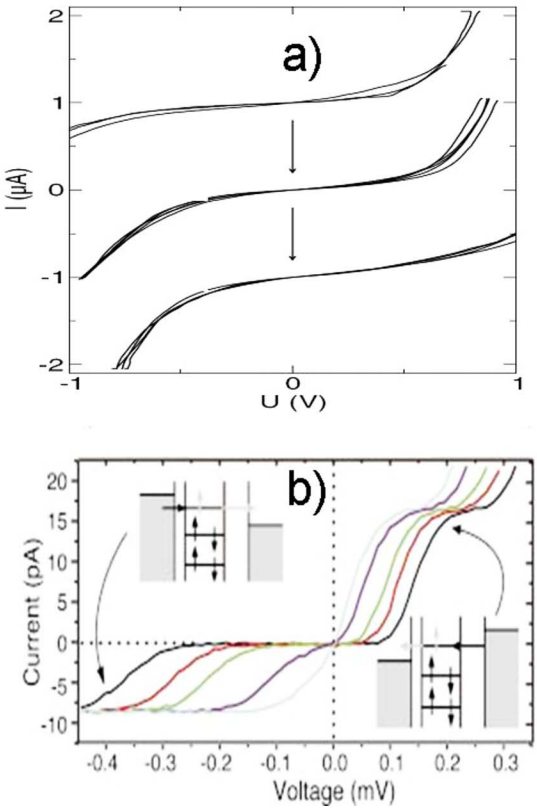


FIG. 1. (Color online) Experiments showing (a) comparable currents reached over unequal voltage widths (Ref. 2) (reprinted with permission) in the SCF limit and (b) unequal currents reached over comparable voltage widths in the CB limit (Ref. 7) (reprinted with permission).

on current rectification frequently observed in molecular dots. In fact, CB asymmetry generates qualitatively different characteristic features compared to SCF asymmetry. We begin by contrasting their separate physical origins and illustrating the crossover from one mechanism to the other in the presence of artificial broadening of the dot levels. A distinct feature of a Coulomb blockaded multiorbital molecular dot is its rich spectrum of electronic excitations that yield unique recognizable transport signatures,[11] consistent with experiments,[3,5,22] such as a gate-dependent exchange of conductance peak asymmetries. We find that the specific identity of these excitations may not be relevant in many cases, allowing us to invoke simpler orthodox models[23–25] that ignore individual excitations in favor of an incoherent sum. Such a coarse-grained CB model can adequately explain multiple experiments,[3,5] considerably reducing the computational cost associated with exactly diagonalizing a many-body Hamiltonian and solving rate equations in its associated Fock space. However, as finally we point out, there are notable exceptions involving specific slow excitation modes or trap states[26–28] that would require careful attention to well-resolved Fock space spectra.

## II. ORIGIN OF ASYMMETRIES—SELF-CONSISTENT FIELD VS COULOMB BLOCKADE

As mentioned earlier, there are two distinct physical limits of transport. In the SCF limit, contact broadenings $\Gamma$ are greater than or comparable to the single electron charging $U$. In the opposite CB limit, $U \gg \Gamma$ and single-electron charging dominates. Conductance asymmetries in both regimes of transport have been experimentally observed in molecular conduction. While there are ways to handle each regime separately, treatments are inherently perturbative, with an approximate treatment of correlation (in terms of $U/\Gamma$) for the SCF regime and an approximate treatment of broadening (in terms of $\Gamma/U$) for the CB regime. The lack of a small parameter in the intermediate coupling regime ($U \sim \Gamma$) makes the exact treatment of transport, even for a simple model system, potentially intractable.[12]

The origin of asymmetric *I-V*'s can be easily elucidated with a minimal model for current conduction through a spin degenerate, filled (closed-shell) molecular doublet. We assume equal *capacitive* couplings but unequal *resistive* couplings to the contacts so that the molecular levels shift by one-half of the applied Laplace potential and the current onsets arise symmetrically around zero bias. In the SCF limit, contact asymmetry results in equal currents adiabatically smeared out over a larger voltage width along one bias direction than the other. This charging based asymmetry has been experimentally seen[2] and can be intuitively rationalized as follows. Consider a spin degenerate energy level, for example, a highest occupied molecular orbital (HOMO), that is fully occupied at equilibrium. For asymmetric contact couplings $\gamma_L \gg \gamma_R$, where $\gamma_L$ and $\gamma_R$ are bare contact couplings to molecular levels, charge addition dominates for positive bias on the right contact and removal for negative bias, as shown in Fig. 2(a). For a positive bias, the energy level is maintained at neutrality by the dominant left contact and the current flow through the level is determined by the removal rate. Along the reverse bias, in contrast, charge removal by the left contact drives the system away from neutrality toward a net positive charge, whose Coulomb cost floats the

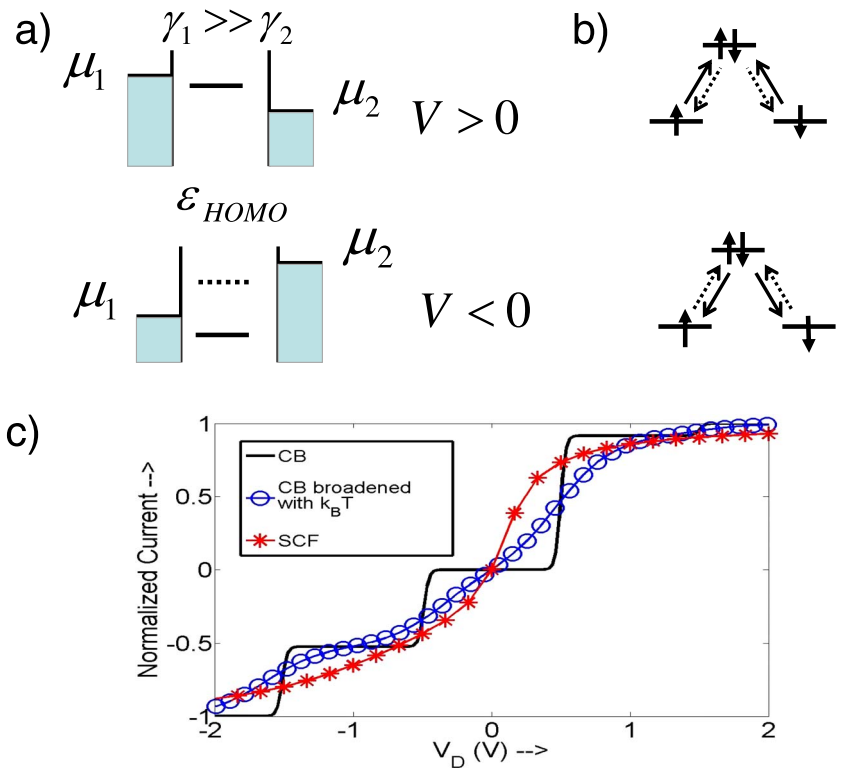


FIG. 2. (Color online) Crossover between asymmetries. An SCF current asymmetry arises for $\gamma_L \gg \gamma_R$ when under positive bias the left contact maintains the HOMO level at neutrality during conduction, while for negative bias, the emptied level is expelled from the bias window by (a) charging and (c) creating *unequal plateau widths* for opposite bias (stars). In the CB regime, however, charge removal by the negatively biased right contact is rate determining and occurs in two different ways, while for positive bias, (b) charge addition is rate determining and can occur in only one way. (c) This leads to an *asymmetry* in plateau heights (bold solid line). While the transition between the two limits is hard to model accurately, (c) a phenomenological broadening through an artificial enhanced temperature circles) illustrates how the open-shell CB plateau morphs into a higher effective broadening, *restoring* the SCF result in the limit of large broadening.

level out of the bias window. This means that a larger bias is needed to fully conduct through the level, dragging out *I-V* in that direction. The direction of asymmetry flips if conduction is instead through the lowest unoccupied molecular orbital. Notably, the maximum currents and their onsets are the same, but their complete saturations are delayed differently for opposite bias directions.

The origin and manifestation of current asymmetry is qualitatively different in the CB limit, where charge addition or removal is abrupt and in integer amounts. Given the asymmetric contact couplings ($\gamma_L \gg \gamma_R$), the left contact adds (removes) an electron as soon as the right contact removes (adds) it, so that the rate determining step becomes the dynamics of the weaker right contact. For a positive bias, charge removal can happen in two ways, from $\uparrow\downarrow$ to $\uparrow$ and $\downarrow$, while for opposite bias the right contact can add a spin in only one way, either $\uparrow$ or $\downarrow$ to $\uparrow\downarrow$. This scheme of charge transfer [Fig. 2(b)] leads to twice the current step for positive bias than for the negative bias.[7,15]

An important issue is whether one can smoothly transition from the CB to the SCF asymmetry by progressively increasing the broadening. While this is hard to do exactly, owing to the inherent difficulty of broadening many-particle states,[29] for the purpose of illustration, one can add broadening to various degrees approximately.[30] We choose to do this by increasing the temperature, which we incorporate through Boltzmann factors in the many-body occupancies.[31] As seen in Fig. 2(c), this approximate treatment morphs the CB asymmetry into the very different version corresponding to the SCF limit. For a negative bias on the weaker contact, "shell filling"[32] of the HOMO level with a net positive charge creates a CB plateau that is missing in its positive bias "shell-tunneling" counterpart. Upon strong coupling with contacts, this one-sided CB plateau merges into a larger broadening manifold, leading to the postponed conduction seen in the SCF limit. It is worth mentioning though that the crossover described is only qualitative and is inaccurate at higher bias values, underscoring the inadequacy of thermal effects and other phenomenological broadening approximations for correlated systems, particularly near the equal coupling, nonequilibrium limit which combines shell tunneling with shell filling.

## III. COULOMB BLOCKADE FORMALISM: FOCK SPACE VS ORTHODOX

In this paper, we focus mainly on the CB regime. Here, one needs to keep track not only of various ground state charge configurations but also of various excitations within each charge state. Exactly diagonalizing the molecular many-body Hamiltonian yields a large spectrum of closely spaced excitations in every charged molecular configuration. The

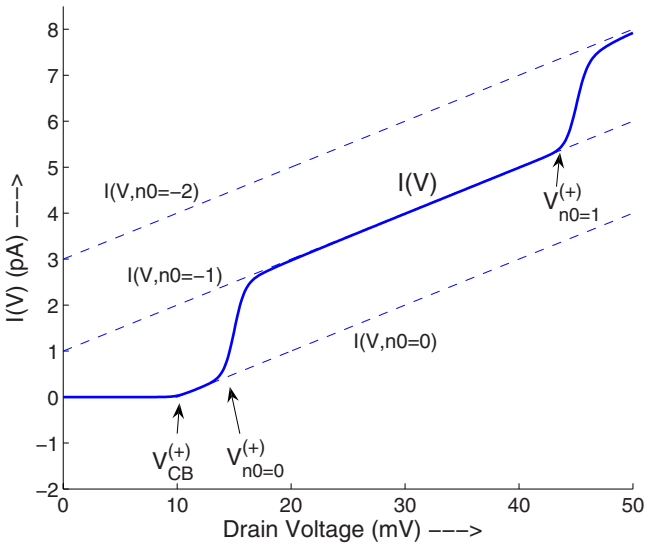


FIG. 3. (Color online) Illustration of orthodox model: The orthodox theory parameters define a set of $I(V,n_0)$ curves, represented by the dashed lines. Starting with $n_0=0$, the current follows the $I(V,n_0=0)$ curve under bias until $n_0$ changes. If $|V_{\mathrm{CB}}|<|V_{n_0=0}|$, as is the case here, the current will rise linearly out of the zero-conductance region; otherwise, there will be a jump onset. For this simulation, $R_1=10$ MΩ, $R_2=6$ GΩ, $C_1=8$ aF, $C_2=5.3$ aF, $Q_0=0$, and $T=2$ K.

current is obtained by solving a set of master equations[14,15,33,34] for the probabilities $P_i^N$ of each $N$ electron many-body state $|N,i\rangle$, giving us

$$I = \pm \frac{e}{\hbar}\sum_{N,ij}[R^{(1)}_{(N,i)\to(N\pm1,j)}P_i^N - R^{(1)}_{(N\pm1,j)\to(N,i)}P_j^{N\pm1}], \quad (1)$$

where $R^{(1)}$ describes the left contact contributions to the many-body transition rates $R$. The computational complexity arises from the need to keep track of not only charge $N$ but also all configurational degrees of freedom $i$. The orthodox model arises by integrating all excitations in an incoherent way,[23–25,35,36] giving us

$$I = \pm \frac{e}{\hbar}\sum_{N}[R^{(1)}_{N\to N\pm1} - R^{(1)}_{N\to N\mp1}]P^N \quad (2)$$

$$= \pm \frac{e}{\hbar}\sum_{N}[R^{(2)}_{N\to N\mp1} - R^{(2)}_{N\to N\pm1}]P^N. \quad (3)$$

The considerably simplified transition rates now depend only on the transition energies that arise just from simple electrostatics in terms of $C_{1,2,G}$ and $C_\Sigma$ (capacitances of contacts 1, 2, and gate and the total capacitance, respectively). For a strong asymmetry of contact resistances ($R_2 \gg R_1$) at low temperatures, the ensemble distribution of electrons on the middle electrode can be described by a delta function $\delta_{n,n_0}$, where $n_0$ is the most probable number of electrons.[25] The delta function probability density reduces Eq. (3) to $I(V_D,V_G)=e/\hbar[R^{(2)}_{n_0\to n_0\mp1}-R^{(2)}_{n_0\to n_0\pm1}]$. For low bias, the Coulomb cost of electron tunneling across the contacts is high, resulting in a zero-conductance region limited by the positive and negative threshold voltages $V_{\mathrm{CB}}^{(+)}$ and $V_{\mathrm{CB}}^{(-)}$, respectively (Fig. 3). Outside of this region, the transition rates simplify to

$$I(V_D,V_G) = \frac{1}{R_2C_\Sigma}\left[-(n_0e-Q_0)+C_1V_D-C_GV_G - \frac{e}{2}\mathrm{sgn}(V_D-V_{\mathrm{CB}}^{(-)})\right], \quad (4)$$

where sgn denotes the Heaviside sign function and $n_0$ is the equilibrium fractional offset charge.[25] The linearity of Eq. (4) with drain voltage is only interrupted when new levels enter into the bias window, causing $n_0$ to change by $\pm1$, which in turn causes the current to "jump" in value.

We thus have an intuitive picture of how $I-V_D$ curves are constructed in the orthodox theory. For given system parameters ($R$, $C$, etc.) and gate voltage, there is a set of $I(V,n_0)$ curves for different values of $n_0$, as dictated by Eq. (4) (e.g., dashed lines in Fig. 3). As a drain voltage is applied, $I(V)$ remains on the $I(V,n_0=0)$ curve until $n_0$ changes, at which point $I(V)$ jumps to the $I(V,n_0=\pm1)$ curve. Generalizations of Eqs. (5) and (6a) from Ref. 25 establish the Coulomb blockade *threshold voltages*,[37]

$$V_{\mathrm{CB}}^{(\pm)} = C_1^{-1}(\pm e/2 - n_0e + Q_0 + C_GV_G), \quad (5)$$

as well as the *transition voltages* between $n_0$ and $n_0\pm1$,

$$V_{n_0}^{(\pm)} = C_2^{-1}(\pm e/2 + n_0e - Q_0 - C_GV_G). \quad (6)$$

In Fig. 3, for example, we can see that the CB threshold voltage is reached at 10 mV, before transition at 15 mV, resulting in a linear onset of the current. If, however, $|V_{n_0}^{(\pm)}|$ were smaller than $|V_{\mathrm{CB}}^{(\pm)}|$, then there would be a jump onset at the zero-conductance region threshold.

Let us now compare the orthodox and Fock-space model approaches to transport in the CB regime and apply them within the context of experimental trends.

## IV. COULOMB BLOCKADE ASYMMETRIES: GATE-DEPENDENT RECTIFICATION

One of the simplest consequences of asymmetric contact coupling is rectification; in other words, a bias direction dependence in the *I-V* characteristics. To calibrate with experiments, we not only concern ourselves with rectification *per se* but also with how it is influenced by a gate. In fact, experiments showcase gate dependences of the rectification properties that are arguably more interesting than the rectifications themselves. These experiments (see, for example, Refs. 3 and 4) show a gate-dependent *shift* of conductance peak onsets, as well as a gate *modulation* of the corresponding conductance peak heights. In addition, there is a prominent *exchange* in conductance peak asymmetry for gate voltage variations about the charge degeneracy point in the stability diagram.[4] We will argue that much of the relevant physics has to do with the way the molecule accesses various electronic excitations under bias, which would require going beyond our one-orbital model to a multiorbital system. Charge addition or removal causes jumps in *I-V*, while

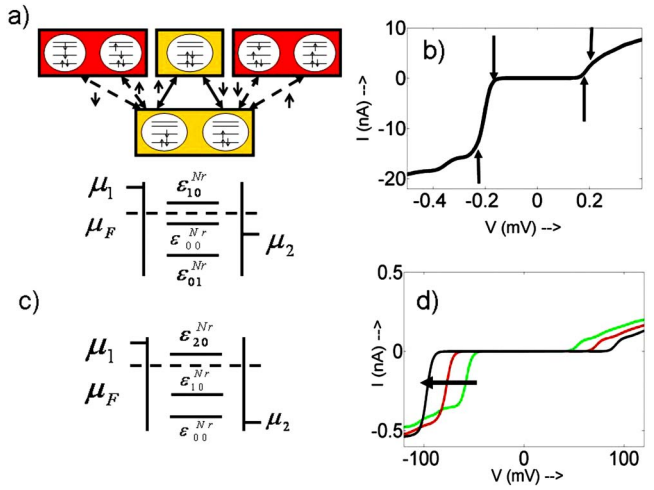


FIG. 4. (Color online) Origin of peak asymmetry and variation with gate voltage. (a) For gate voltages that place the contact Fermi energy $\mu_F$ in the $N$ electron blockade region, the levels align such that $\mu_F > \epsilon_{00}^{Nr}$. A state transition diagram shows the addition and removal of up (down) spins resulting in transitions $\epsilon_{00}^{Nr}$ (bold double arrow) between ground states of neutral and positively charged species (light orange). Also shown in the state transition diagram are transitions (dashed double arrow) between various configurations of neutral excited state (deep orange) and positively charged ground state, labeled $\epsilon_{10}^{Nr}$. (c) The resulting $I$-$V$ shows clear asymmetry in the peak height due to there being more ways to add an electron. (c) Increasing gate voltage increases the number of excitations available, giving a pronounced (d) current height modulation with gate voltage. The inset shows the corresponding $I$-$V$ characteristics (Refs. 3, 4, and 11).

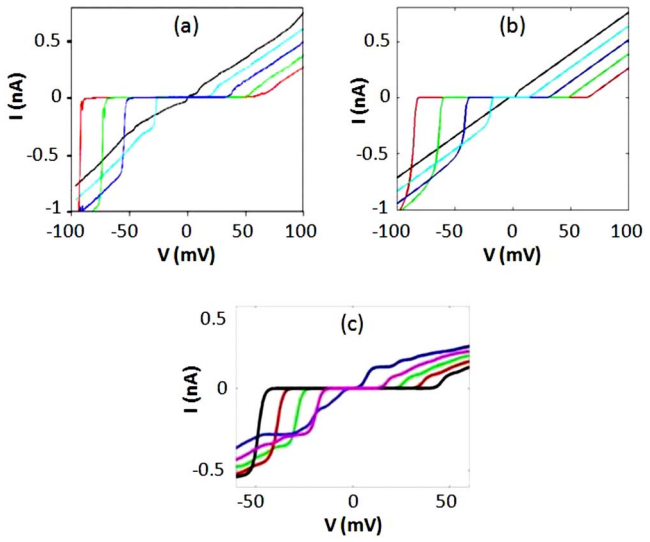


FIG. 5. (Color online) Experiment from Park *et al.* (Ref. 3) showing gate-rectification properties in the Coulomb blockade regime: (a) experimental traces (reprinted with permission), (b) orthodox fit with parameters $C_1$=0.624 aF, $C_2$=0.486 aF, $C_G$ =0.0708 aF, $R_1$=1 MΩ, $R_2$=75 MΩ, $Q_0$=−0.05$e$, and $T$=2.2 K, and (c) fit from Fock-space model.

charge redistribution (excitation) leads to closely spaced plateaus that merge onto a linear ramp when summed incoherently. In the rest of the section, we will explain how each CB model (Fock space and orthodox) successfully captures the gate modulation of the asymmetric $I$-$V$'s, as summarized schematically in Figs. 4 and 7.

### A. Gate modulation of current onsets and heights

The onset of conduction is determined by the offset between the equilibrium Fermi energy and the first accessible transition energy, marked $\epsilon_{00}^{Nr}$ in Fig. 4 (following the nomenclature in Sec. II). This can be modified by varying the gate voltage, thereby accounting for the variation in conductance gap with gate voltage [Fig. 4(c)]. While the current step and corresponding conductance peak are generated by this threshold transition, there follows a quasi-Ohmic rise in current, leading to a subsequent constant nonzero conductance in the conductance-voltage ($G$-$V$) characteristics. This feature arises from the sequential access of several closely spaced transport channels under bias due to excitations within the $N$ and $N-1$ electron subspaces.[11] While net charge addition and removal come at large Coulomb prices, excitations involve charge reorganization within the Fock space that cost much smaller correlation energies.

The presence of multiple orbitals generates several configurations of excited states, creating more accessible transport channels within the bias window. For example, in Fig. 4(a), conduction occurs simultaneously via the $\epsilon_{10}^{Nr}$ and $\epsilon_{00}^{Nr}$ removal channels. $\epsilon_{10}^{Nr}$ corresponds to a transition between the first excited state "1" of the $N$-electron neutral species and the ground state "0" of the $N-1$ electron cationic species. We show four possible configurations corresponding to the transport channel $\epsilon_{10}^{Nr}$ and the corresponding $I$-$V$ [Fig. 4(b)]. Increasing the gate voltage increases both the threshold for current conduction and the number of such excited state channels accessed by the contacts, thereby altering the height of the corresponding conductance peak with gate voltage [Fig. 4(c)].

The previous paragraph illustrates the origin of gate-modulated current as rationalized by the *Fock-space CB model*. One can also explain this within the simpler *orthodox model*, which ignores the identities of the resolved excitations by incoherently summing them. Under the approximations of contact asymmetry and low temperature, the rate $R_{N\to N\pm1}^{(j)}$ is linear in the transition energies $\Delta E_j^{\pm}$ that increase with drain voltage. With increasing gate voltage, one needs a larger corresponding drain bias to overcome the zero-conductance regime. At this higher drain voltage, the coupling has a greater value and, consequently, the current magnitude is larger. Physically, the drain voltage dependence of the coupling represents a linear approximation of the excitation spectra. Even though the orthodox model indiscriminately sums the excitations within the $N$ and $N-1$ subspaces, the fact that it captures them at all allows it to qualitatively capture the modulation of current height.

Figures 5(a) and 6(a) show the experimental evidence of gate modulation of current onsets and heights. Figure 5(a) shows an experiment for which the negative bias onset is set by moving from the $N$ to $N-1$ electron subspace, while the positive bias onset starts where the $N$ electron excitation

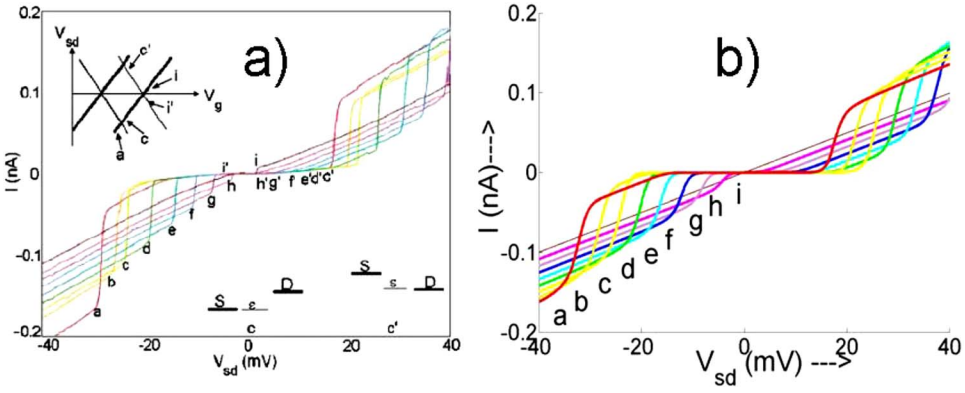


FIG. 6. (Color online) Asymmetric CB results showing (a) experiment (Ref. 5) (reprinted with permission) and (b) orthodox theory with parameters $C_1=3.70$ aF, $C_2=3.24$ aF, $C_G=0.061$ aF, $R_1=2$ MΩ, $R_2=210$ MΩ, $Q_0=0.175e$, and $T=4.2$ K.

spectrum moves into the bias window. Figures 5(b) and 5(c) show the abilities of both the orthodox model and the Fock-space model to capture the gate-modulated features of the experiment. Figure 6(a) shows a similar experiment with slightly more complex features. Curves d–h show the same negative bias onset, as seen in Fig. 5, but as the gate voltage is further decreased, the negative onset changes to a linear onset, representing access to the $N$ electron excitation spectrum. The positive bias shows that decreasing gate voltage brings the $N+1$ level closer to the bias window. For curves a–c, the positive bias type consequently becomes a jump onset. In spite of these new degrees of freedom that must be captured, the orthodox theory works quite effectively, as seen in Fig. 6(b). It is worth noting that the $x$ axis in Fig. 6 is $V_{SD}$, rather than $V_{DS}$, which must be accounted for when using Eqs. (5) and (6) of the orthodox theory.

Mathematically, it is straightforward to understand the dependence of current height on gate voltage within the orthodox theory. Using the experiment of Park *et al.*[3] [Fig. 5(a)] as an example, we see that there is a jump onset for negative bias voltages. Therefore, $|V_{n_0}^{(-)}|<|V_{\mathrm{CB}}^{(-)}|$. At $V_{n_0}^{(-)}$, the $I$-$V$ transitions to the $I(V,n_0=-1)$ curve. So, to find the current height at the onset voltage, we can use Eq. (4) for $n_0=-1$. Inserting $V_{n_0}^{(-)}$ for $V_D$, one finds

$$I(V_{n_0}^{-}) = -\frac{C_1+C_2}{R_2C_2C_\Sigma}(Q_0+e/2+C_GV_G). \tag{7}$$

Clearly, the magnitude of the current at the onset voltage increases with gate voltage [Fig. 5(b)], matching the experimental result seen in Fig. 5(a).

The accuracy of the orthodox simulation would imply at the very least that individual excitations do not play an important role in the transport characteristics seen. Because the experimental $I$-$V$ has a strongly linear dependence on drain voltage seen in Eq. (4), it seems that the experiments may have measured transport through a metallic particle, which has a relatively featureless density of states, as assumed in the orthodox model.

### B. Peak exchange

Experiments exhibit a characteristic flipping of conductance peak asymmetry around the charge degeneracy point A in the stability diagram [Figs. 7(a) and 7(b)]. Figures 7(e) and 7(f) show typical calculated $G$-$V$'s in this regime, featuring conductance peak asymmetries with respect to voltage bias, arising due to asymmetric contact couplings ($\gamma_L \gg \gamma_R$). Within the Fock-space model, this can be explained by enumerating the channels for adding and removing electrons under bias [Figs. 7(b) and 7(d)], with the weaker right contact once again setting the rate limiting step. The dominant transport channel $\epsilon_{00}^{Nr}$ corresponds to electronic transitions between the neutral and cationic ground states,[11] states which SCF theories do take into account. In the CB limit, however, there are additional electronic excitations that are accessible with very little Coulomb cost. These states are responsible for the peak asymmetry exchange observed in these experiments, as we will now explain.

The origin of this asymmetry can be understood with a simple model system: in our case, a quantum dot with eight spin-degenerate levels and $N=4$ electrons in its ground state. When the Fermi energy lies to the immediate right of the charge degeneracy point, as shown in Fig. 7(a), only transitions between the $N$ and $N-1$ electron states (4 and 3) are allowed, with the weaker right contact setting the rate-limiting step. For positive bias on the right contact, an electron can be removed from the four-electron to the three-electron ground state in two ways [Fig. 7(b)]. For a negative bias, however, the electron removed by the left contact can be replenished by the right contact back into the four-electron ground state, and also into one of many possible excited states $\epsilon_{i0}^{4r}=E_i^4-E_0^3$ ($i>0$). Since there are more ways to bring the electron back (six shown here), the conductance is larger for negative bias [Fig. 7(e)]. The situation changes dramatically for a different position of the Fermi energy [Fig. 7(c)] in the stability diagram lying to the left of the charge degeneracy point A with three electrons at equilibrium. For a positive bias, the right contact adds an electron from the three- to the four-electron ground state, while for a negative bias, it returns it to the $j$th three-electron excited state through transitions $\epsilon_{0j}^{4r}=E_0^4-E_j^3$. Now, there are more ways to remove than add a charge [Fig. 7(d)], so that the asymmetry flips [Fig. 7(f)].

Analogous to the Fock-space model, the orthodox model also captures gate-dependent peak exchange, in spite of its approximate treatment of excitations. The origin of the asymmetry is once again the transition between the $N$ to $N-1$ electron regimes. In Fig. 3, we can see that such a change results in a jump onset that has a much higher conductance

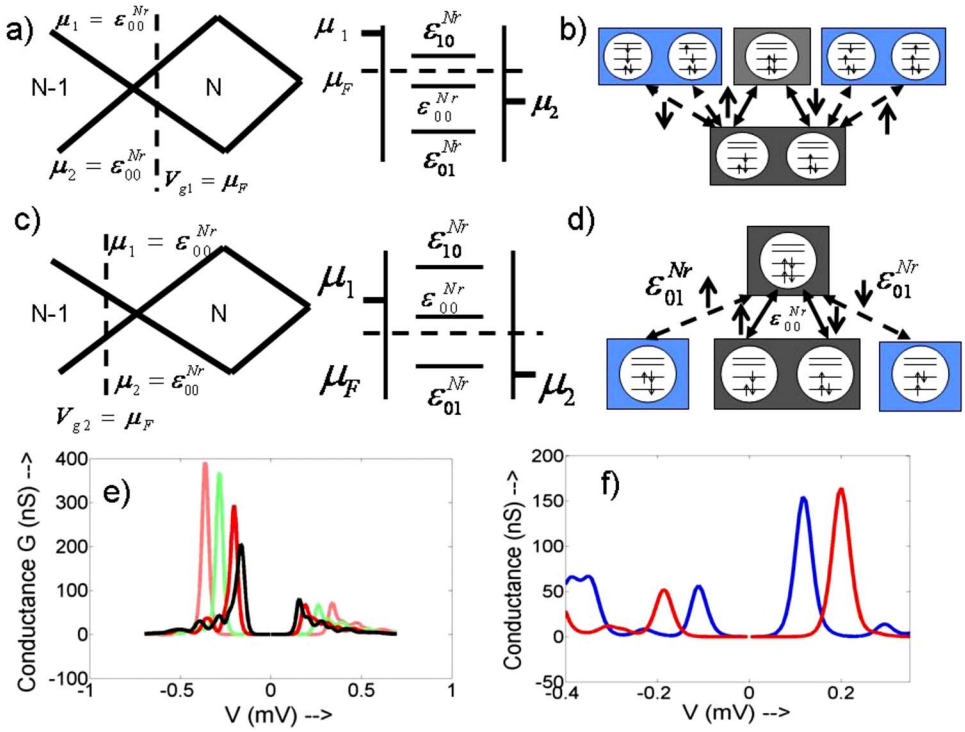


FIG. 7. (Color online) Origin of exchange in asymmetry of conductance peaks: (a) and (b) Schematic of vicinity of charge degeneracy point A in Coulomb diamond. Also shown are the corresponding energy diagrams at threshold. Notice a different set of threshold transport channels between (a) and (b). (c) and (d) State transition diagrams illustrating the different excitation spectra accessed on either side of the charge degeneracy point A. (e) and (f) $G$-$V$ plots for scenarios (a) and (b). Notice the clear peak exchange as a result of accessing different excitation spectra in either case.

value than a linear onset. Moving from the $I(V,n_0)$ curve to the $I(V,n_0-1)$ curve, therefore, essentially captures the excitations of the $N-1$ electron spectrum that are pivotal to the argument in the preceding paragraph. The fact that the conductance peak switches across zero bias only means that the zero-bias state of the system changes from $N$ to $N-1$ electrons, which the orthodox method clearly captures.

Peak exchange has been reported experimentally,[4] as seen in Fig. 8(a). Figure 8(b) shows an orthodox simulation of the experiment. One can see close qualitative and quantitative agreements between the experimental data and the theoretical simulation. The conductance peaks have similar magnitudes, and the exchange of the peak asymmetry occurs at −3.75 V in both graphs. The evident validity of the orthodox theory in this case demonstrates its ability to capture excitation features, as long as the features can be linearly approximated.

## V. LIMITATIONS OF THE ORTHODOX MODEL

Based on the success of the orthodox model in the previous section, it is tempting to conclude that molecules with redox-active centers only exhibit incoherent superpositions of excitations rather than well-resolved features. In this section, we point out examples where the discrete excitation spectrum can indeed play a noticeable role in molecular transport experiments, making an orthodox theoretical treatment quite inadequate.

Ultrasmall quantum dots can potentially exhibit both charge and size quantizations.[12] While charge quantization shows up through a Coulomb blockade of zero-bias conductances, size quantization manifests as conductance peaks.[38] Other quantum dot experiments routinely show Coulomb diamonds with well-resolved excitation lines,[39] such as those

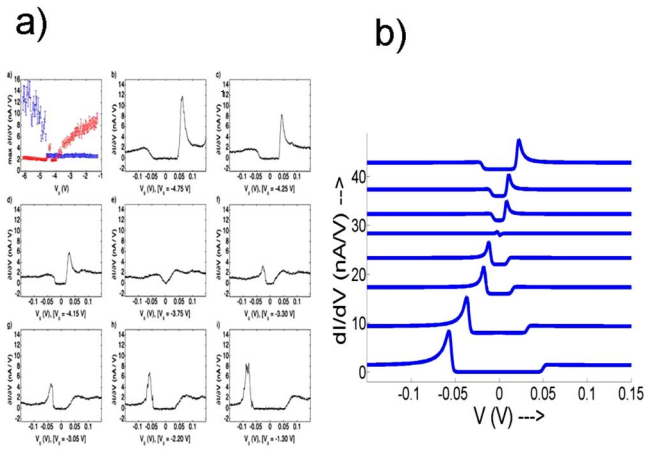


FIG. 8. (Color online) (a) Experimental trace demonstrating peak asymmetry exchange (Ref. 4). Compare with Fock-space model results in Figs. 7(e) and 7(f). (b) Orthodox simulation reproducing peak exchange observed in the experiments. The parameters are $R_1=35$ MΩ, $R_2=350$ MΩ, $C_1=0.673$ aF, $C_2=0.612$ aF, $C_G=0.0135$ aF, $Q_0=-0.18e$, and $T=4.2$ K.

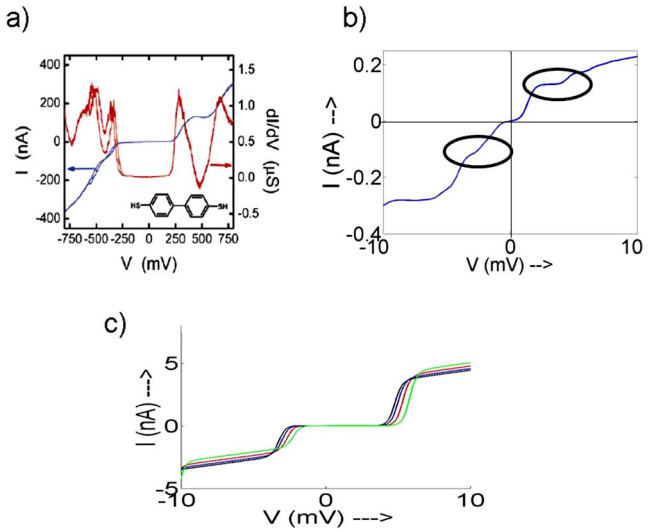


FIG. 9. (Color online) Limitation of orthodox model: (a) Experimental trace (Ref. 22) (reprinted with permission) showing fine structure. (b) The fine structure in *I-V*'s, result from keeping track of excitations explicitly within the Fock-space CB model. (c) An orthodox calculation merely maintains the same slope between charge addition jumps, thus may not reproduce any fine structure.

due to vibronic cotunneling[40] and Kondo resonances,[41] which would require special attention to individual excitations rather than just their incoherent superposition. A recently observed negative differential resistance (NDR) in double quantum dots[26] can, in fact, be explained in terms of a triplet state with a significantly longer lifetime than other states.[20,26] Recent experiments performed on single molecular magnets not only show direct signatures of magnetic excitations[27,28] but also NDR effects due to spin selection rules.[28,42,43]

Signatures of well-resolved excitations occur less frequently in molecules due to their larger vibronic flexibility and broadening, but they do show up occasionally through fine structures in *I-V*, as seen in multiple experiments (see, for example, Ref. 22 reproduced in Fig. 9). For instance, the gap between ground and first excited states, involving charge addition or removal, is significantly greater than the gap between subsequent excitations involving charge reorganization. In such a case, a brief plateau occurs at threshold and persists until the first excitation is accessed, as discussed in detail in Ref. 11. Experiments like these require keeping track of individual molecular excitations using Fock-space CB. The orthodox theory cannot even qualitatively match the experimental data in Fig. 9, owing to its *inability* to incorporate size quantization effects and the associated discrete spectra. From Eq. (4), it is clear that outside of the zero-conductance region and excluding jumps due to changes in $n_0$, conductance values in orthodox theory must remain constant, with a value of $R_1/R_2C_\Sigma$. The orthodox theory can capture a plateau, and it can also capture a linear rise, but it does *not* seem to capture both in the same *I-V* curve. Figure 9(c) shows the best attempt at modeling the experimental data in Fig. 9(a) within the orthodox theory; the plateau followed by a linear rise seems hard to duplicate.

A second limitation of the orthodox model comes in its *treatment of gate voltage*. Even though it effectively modeled

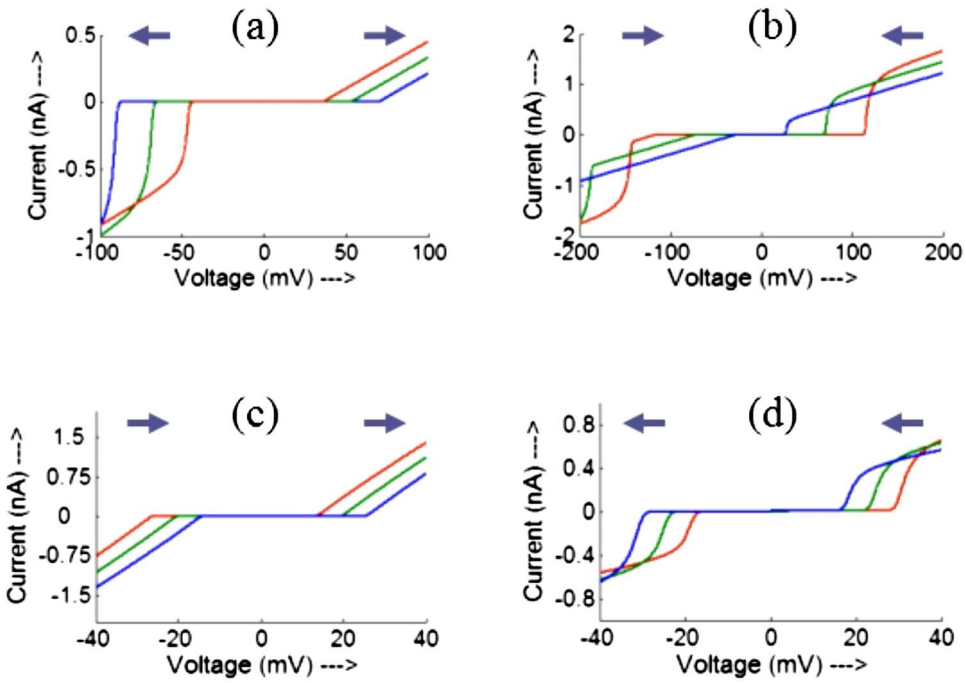


FIG. 10. (Color online) Gate-voltage dependence of *I-V* curves in the orthodox theory. Blue arrows indicate the direction of movement of the onset voltages with increasing gate voltage. The four plots correspond to the four possible onset combinations: (a) a jump onset at negative bias and a linear onset at positive bias, for which the *I-V* conductance gap *widens* with increasing gate voltage; (b) a linear onset then a jump onset, with the gap *narrowing* around zero-bias; (c) two linear onsets, which corresponds to a *translation* of the *I-V* curve: and (d) two jump onsets, which correspond to a translation in the opposite direction of (c).

the data in Figs. 5, 6, and 8, there again exist experimental features that the orthodox theory cannot even qualitatively model. Looking at Eqs. (5) and (6), one can see that a change in gate voltage causes a *translation* in the Coulomb blockade threshold voltages; a similar effect, although in the opposite direction, is seen for the voltage limits at which $n_0$ changes. Figure 10 shows how an orthodox *I-V* curve changes with gate voltage for the four possible onset combinations—which come from having linear or jump onsets at positive and negative biases. The scaling of the conductance gap in Figs. 10(a) and 10(b) successfully explained the experiments in Figs. 5 and 8. However, for experiments with symmetric onsets [Figs. 10(c) and 10(d)], one can see that the orthodox theory predicts an overall translation in the *I-V* curve with gate voltage. One would think that changing the gate voltage would only shift the conducting level closer to or further from the bias window, thereby narrowing or widening the *I-V* curve, respectively. Indeed, experimental evidence demonstrates such narrowing,[7] and the Fock-space model captures that quite easily. The orthodox theory could not match this trend even qualitatively.

## VI. DISCUSSIONS

A proper treatment of individual molecular excitations may seem rather academic at this point; however, there could be important experimental features requiring a proper quantitative theory as transport spectroscopy of molecules becomes feasible.[44] In fact, a possible explanation for molecular NDRs[45,46] could necessitate, keeping track of excitations in a donor-acceptor molecular system.[20] Small molecules could function as tunable quantum dots with high single-electron charging energies. Molecular dots coupled to transistor channels can be important for the detection, characterization, and manipulation of individual spin qubits,[44] with the transistor conductance providing a means of electronic readout.[47] The large charging energies could allow redox-active molecules to operate as storage centers for memory.[48] Rectification could be important in this context to avoid parasitic pathways in cross-bar logic architectures.[49]

The accurate treatment of well-resolved excitations is crucial in the above examples of engineered molecular scattering. The price paid, however, is the loss of simplicity that orthodox theory provided. Instead, we will need a major improvement in computational algorithms to handle the exponential scaling of the Fock space, practical ways to identify the most relevant configuration interaction matrices, inclusion of interference between degenerate states using a density matrix, as well as a formal treatment of broadening of the many-particle states, which can allow nondegenerate states to interfere as well.[29] Needless to say, there is enormous room for theoretical and computational activities in this domain and for novel device operational principles arising out of it.

## VII. CONCLUSION

In this paper, we provided a detailed discussion of transport under contact induced asymmetry, keeping the theoretical interpretation of experimental features in mind. We outlined the different physical origins of asymmetric transport features and the crossover between the NEGF-based SCF limit and the Fock-space-based CB limit. We also showed that although Fock-space CB models allows us to explain the excited state dynamics of a multiorbital molecular dot and various transport signatures[11] seen in notable experiments,[3] such characteristic CB signatures, namely, gate dependent conductance peaks and the flipping of their asymmetry, can, in fact, be explained with a simpler "orthodox" model[23–25] as well. This model ignores individual excitations in favor of an incoherent sum. This approach is extremely advantageous as opposed to the computationally intensive Fock-space approach based on an exact diagonalization of a many-body Hamiltonian. Finally, the limitations of such a simplification were discussed using notable exceptions to well-resolved Fock space excitation spectra that need careful attention.

## ACKNOWLEDGMENTS

We would like to thank S. Datta, L. Harriott, G. Scott, and H.-W. Jiang for useful discussions. This project was supported by the DARPA-AFOSR grant.

[1] A. Aviram and M. A. Ratner, Chem. Phys. Lett. **29**, 277 (1974).
[2] J. Reichert, R. Ochs, D. Beckmann, H. B. Weber, M. Mayor, and H. v. Löhneysen, Phys. Rev. Lett. **88**, 176804 (2002).
[3] J. Park, A. N. Pasupathy, J. I. Goldsmith, C. Chang, Y. Yaish, J. R. Petta, M. Rinkovski, J. P. Sethna, H. D. Abruna, P. L. McEuen, and D. C. Ralph, Nature (London) **417**, 722 (2002).
[4] G. D. Scott, K. S. Chichak, A. J. Peters, S. J. Cantrill, J. F. Stoddart, and H. W. Jiang, Phys. Rev. B **74**, 113404 (2006).
[5] N. B. Zhitenev, H. Meng, and Z. Bao, Phys. Rev. Lett. **88**, 226801 (2002).
[6] F. Zahid, M. Paulsson, A. W. Ghosh, E. Polizzi, and S. Datta, Phys. Rev. B **70**, 245317 (2004).
[7] M. M. Deshmukh, E. Bonet, A. N. Pasupathy, and D. C. Ralph, Phys. Rev. B **65**, 073301 (2002).
[8] S. Datta, *Quantum Transport: Atom to Transistor* (Cambridge University Press, New York, 2005).
[9] R. Asgari, Solid State Commun. **141**, 563 (2007).
[10] P. S. Damle, A. W. Ghosh, and S. Datta, Chem. Phys. **281**, 171 (2002).
[11] B. Muralidharan, A. W. Ghosh, and S. Datta, Phys. Rev. B **73**, 155410 (2006).
[12] B. Muralidharan, A. W. Ghosh, and S. Datta, Mol. Simul. **32**, 751 (2006).
[13] B. Muralidharan, A. W. Ghosh, S. K. Pati, and S. Datta, IEEE Trans. Nanotechnol. **6**, 536 (2007).
[14] M. H. Hettler, W. Wenzel, M. R. Wegewijs, and H. Schoeller, Phys. Rev. Lett. **90**, 076805 (2003).
[15] E. Bonet, M. M. Deshmukh, and D. C. Ralph, Phys. Rev. B **65**,

045317 (2002); C. W. J. Beenakker, *ibid.* **44**, 1646 (1991).
[16] M. Koentopp, K. Burke, and F. Evers, Phys. Rev. B **73**, 121403(R) (2006).
[17] J. J. Palacios, Phys. Rev. B **72**, 125424 (2005).
[18] C. Toher, A. Filippetti, S. Sanvito, and K. Burke, Phys. Rev. Lett. **95**, 146402 (2005).
[19] M. Elbing, R. Ochs, M. Koentopp, M. Fischer, C. von Hanish, F. Weigend, F. Evers, H. B. Weber, and M. Mayor, Proc. Natl. Acad. Sci. U.S.A. **102**, 8815 (2005).
[20] B. Muralidharan and S. Datta, Phys. Rev. B **76**, 035432 (2007).
[21] L. Siddiqui, A. W. Ghosh, and S. Datta, Phys. Rev. B **76**, 085433 (2007).
[22] J.-O. Lee, G. Lientschnig, F. Wiertz, M. Struijk, R. A. J. Janssen, R. Egberink, D. N. Reinhoudt, P. Hadley, and C. Dekker, Nano Lett. **3**, 113 (2003).
[23] *Single Charge Tunneling*, NATO ASI Series B: Physics, edited by H. Grabert and M. H. Devoret (Plenum, New York, 1992), Vol. 294.
[24] M. Amman, R. Wilkins, E. Ben-Jacob, P. D. Maker, and R. C. Jaklevic, Phys. Rev. B **43**, 1146 (1991).
[25] A. E. Hanna and M. Tinkham, Phys. Rev. B **44**, 5919 (1991).
[26] K. Ono, D. G. Austing, Y. Tokura, and S. Tarucha, Science **297**, 1313 (2002).
[27] See, for example, M-H. Jo, J. E. Grose, K. Baheti, M. M. Deshmukh, J. J. Sokol, E. M. Rumberger, D. N. Hendrickson, J. R. Long, H. Park, and D. C. Ralph, Nano Lett. **6**, 2014 (2006).
[28] H. B. Heersche, Z. de Groot, J. A. Folk, H. S. J. van der Zant, C. Romeike, M. R. Wegewijs, L. Zobbi, D. Barreca, E. Tondello, and A. Cornia, Phys. Rev. Lett. **96**, 206801 (2006).
[29] J. N. Pedersen and A. Wacker, Phys. Rev. B **72**, 195330 (2005).
[30] K. M. Indlekofer, J. Knoch, and J. Appenzeller, IEEE Trans. Electron Devices **54**, 1502 (2007).
[31] G. Klimeck, G. L. Chen, and S. Datta, Phys. Rev. B **50**, 2316 (1994).
[32] F. P. A. M. Bakkers, Z. Hans, A. Zunger, A. Franceschetti, L. P. Kouwenhoven, L. Gurevich, and D. Vanmaekelbergh, Nano Lett. **1**, 551 (2001).
[33] F. Elste and C. Timm, Phys. Rev. B **71**, 155403 (2005).
[34] S. Braig and P. W. Brouwer, Phys. Rev. B **71**, 195324 (2005).
[35] D. V. Averin, A. N. Korotkov, and K. K. Likharev, Phys. Rev. B **44**, 6199 (1991).
[36] V. V. Shorokhov, P. Johansson, and E. S. Soldatov, J. Appl. Phys. **91**, 3049 (2002).
[37] Note that the signs of $n_0$ and $Q_0$ in the following equations will differ from those in Ref. 25 because we are using a negative charge carrier convention.
[38] U. Banin, Y. Cao, D. Katz, and O. Millo, Nature (London) **400**, 542 (1999).
[39] See, for example, S. Sapmaz, P. Jarillo-Herrero, J. Kong, C. Dekker, L. P. Kouwenhoven, and H. S. J. van der Zant, Phys. Rev. B **71**, 153402 (2005) and references therein.
[40] S. DeFranceschi, S. Sasaki, J. M. Elzerman, W. G. van der Wiel, S. Tarucha, and L. P. Kouwenhoven, Phys. Rev. Lett. **86**, 878 (2001).
[41] D. Goldhaber-Gordon, H. Shtrikman, D. Mahalu, D. Abusch-Magder, U. Meirav, and M. A. Kastner, Nature (London) **391**, 156 (1998).
[42] C. Romeike, M. R. Wegewijs, and H. Schoeller, Phys. Rev. Lett. **96**, 196805 (2006).
[43] D. Weinmann, W. Häusler, and B. Kramer, Phys. Rev. Lett. **74**, 984 (1995).
[44] M. Xiao, I. Martin, E. Yablonovitch, and H. W. Jiang, Nature (London) **430**, 435 (2004).
[45] J. Chen, M. A. Reed, A. M. Rawlett, and J. M. Tour, Science **286**, 1550 (1999).
[46] R. A. Kiehl, J. D. Le, P. Candra, R. C. Hoye, and T. R. Hoye, Appl. Phys. Lett. **88**, 172102 (2006).
[47] F. H. L. Koppens, C. Buizert, K. J. Tielrooij, I. T. Vink, K. C. Nowack, T. Meunier, L. P. Kouwenhoven, and L. M. K. Vandersypen, Nature (London) **442**, 766 (2006).
[48] Q. Li, S. Surthi, G. Mathur, S. Gowda, Q. Zhao, T. A. Sorensen, R. C. Tenent, K. Muthukumaran, J. S. Lindsey, and V. Misra, Appl. Phys. Lett. **85**, 1829 (2004).
[49] M. Stan, P. Franzon, S. Goldstein, J. Lach, and M. Ziegler, Proc. IEEE **91**, 1940 (2003).